Electronic Supplementary Material (ESI) for Nanoscale.

Supporting Information

Fabrication of nanosheet-assembled hollow copper-nickel phosphide spheres embedded in reduced graphene oxide texture for hybrid supercapacitors

Maryam Amiri, Akbar Mohammadi Zardkhoshoui* and Saied Saeed Hosseiny Davarani*

Department of Chemistry, Shahid Beheshti University, G. C., 1983963113, Evin, Tehran, Iran.
Corresponding authors: *Tel: +98 21 22431661; Fax: +98 21 22431661; E-mail: ss-hosseiny@sbu.ac.ir (S.S.H. Davarani); and mohammadi.bahadoran@gmail.com (A. Mohammadi Zardkhoshoui)

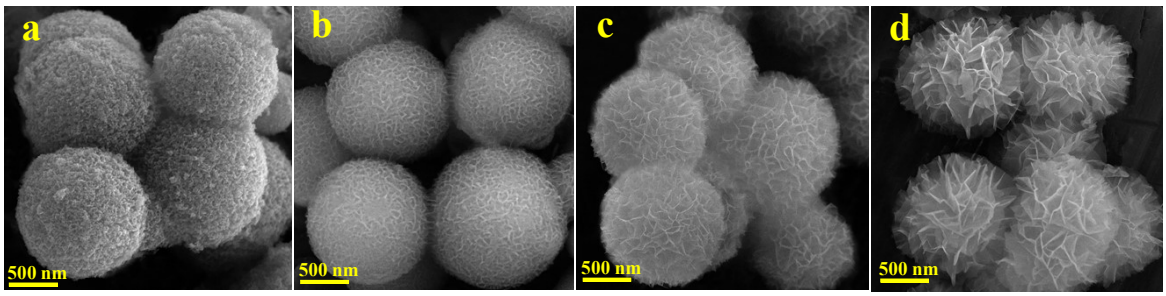

Fig. S1 (a) FE-SEM image of the CN-EG32-100. (b) FE-SEM image of the CN-EG32-130. (c) FE-SEM image of the CN-EG32-160. (d) FE-SEM image of the CN-EG32-180.

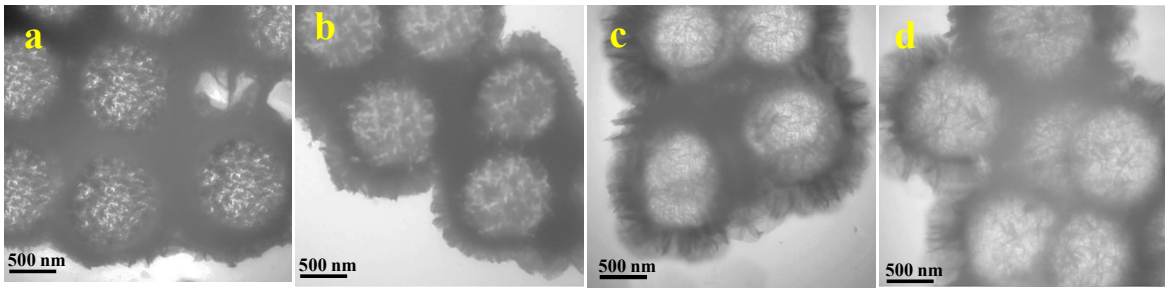

Fig. S2 (a) TEM image of the CN-EG32-100. (b) TEM image of the CN-EG32-130. (c) TEM image of the CN-EG32-160. (d) TEM image of the CN-EG32-180.

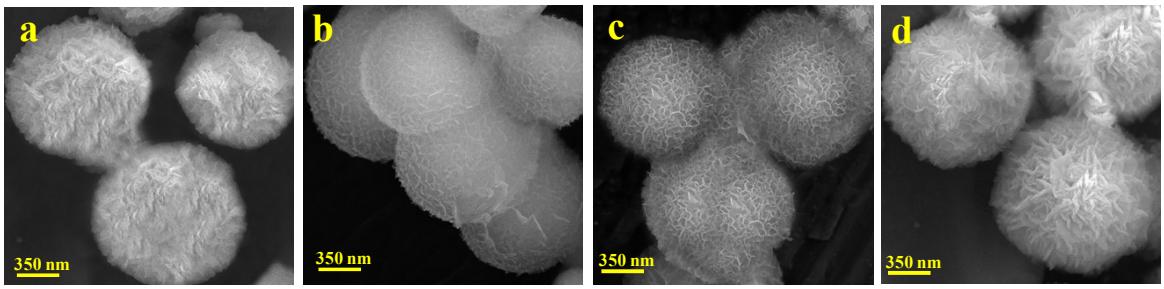

Fig. S3 (a) FE-SEM image of the CN-EG11-180. (b) FE-SEM image of the CN-EG12-180. (c) FE-SEM image of the CN-EG21-180. (d) FE-SEM image of the CN-EG23-180.

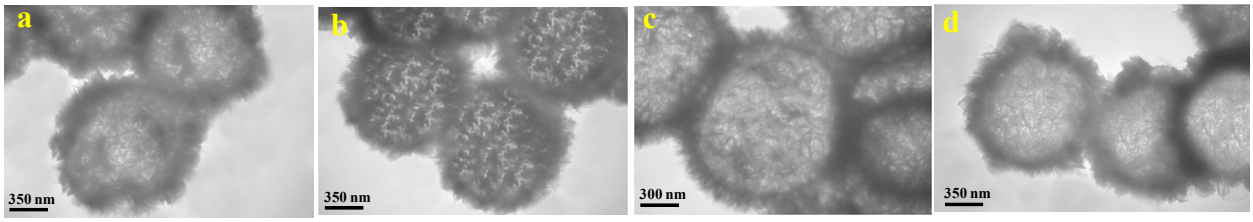

Fig. S4 (a) TEM image of the CN-EG11-180. (b) TEM image of the CN-EG12-180. (c) TEM image of the CN-EG21-180. (d) TEM image of the CN-EG23-180.

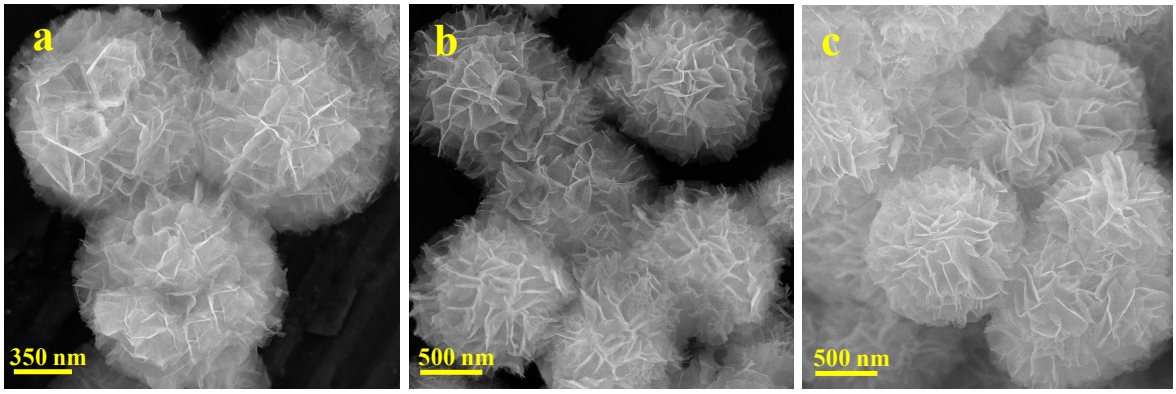

Fig. S5 (a) FE-SEM image of the NH-CNPS-150. (b) FE-SEM image of the NH-CNPS-250. (c) FE-SEM image of the NH-CNPS-450.

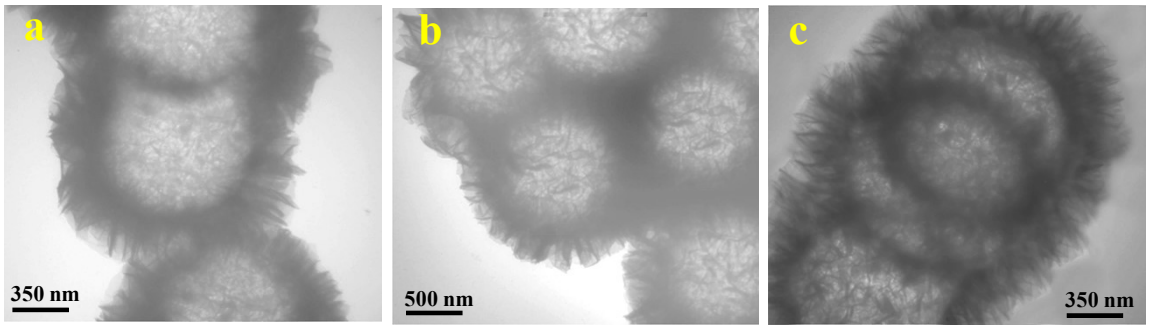

Fig. S6 (a) TEM image of the NH-CNPS-150. (b) TEM image of the NH-CNPS-250. (c) TEM image of the NH-CNPS-450.

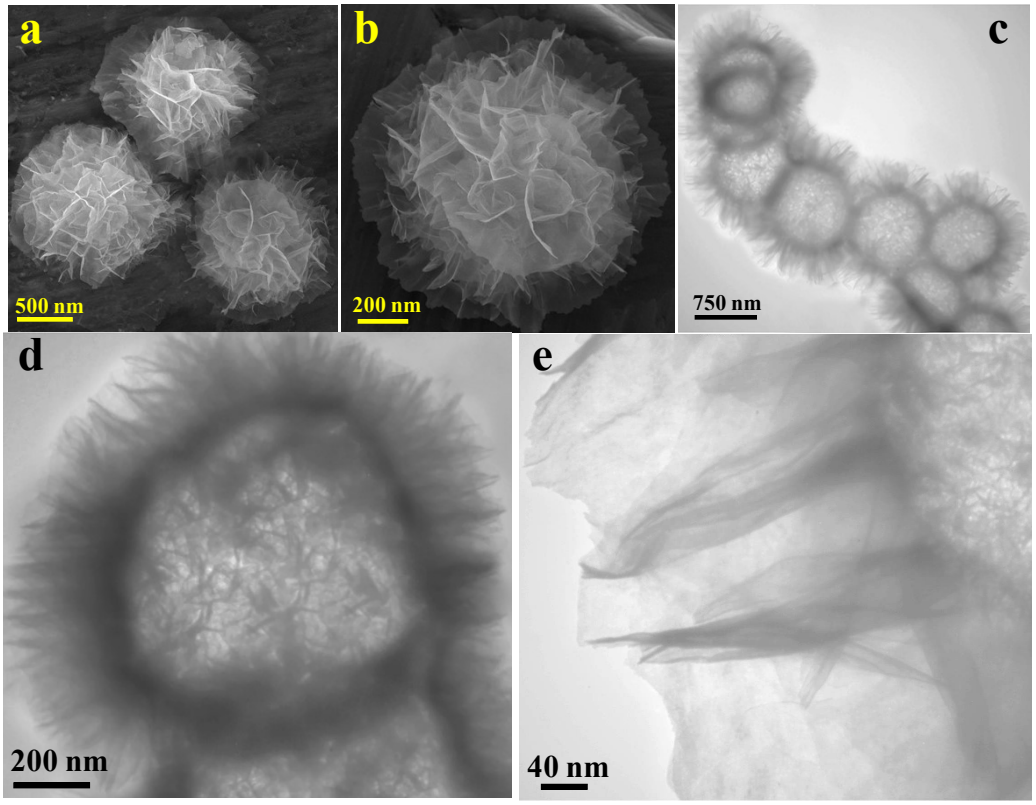

Fig. S7 (a, b) FE-SEM images of the NH-CNPS-350. (c-e) TEM images of the NH-CNPS-350.

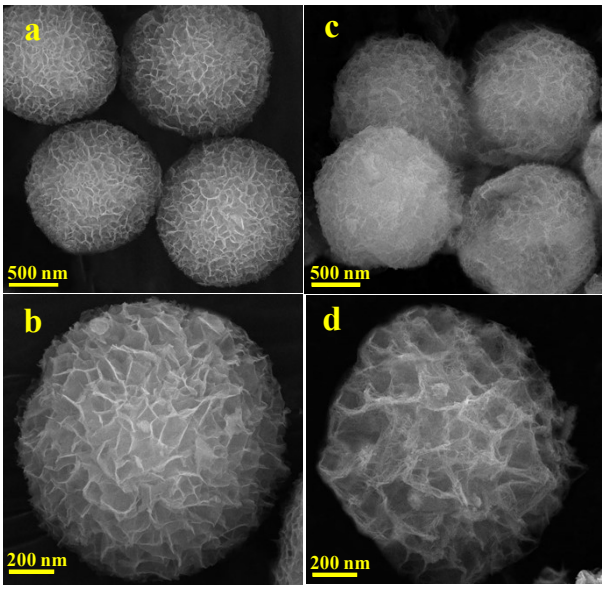

Fig. S8 (a, b) FE-SEM images of the single Cu_3P. (c, d) FE-SEM images of the single Ni_2P.

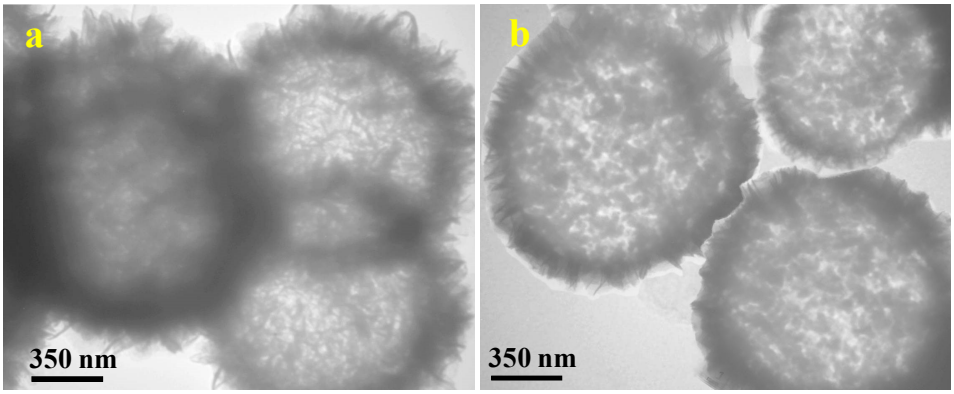

Fig. S9 (a) TEM image of the single Cu_3P. (b) FE-SEM image of the single Ni_2P.

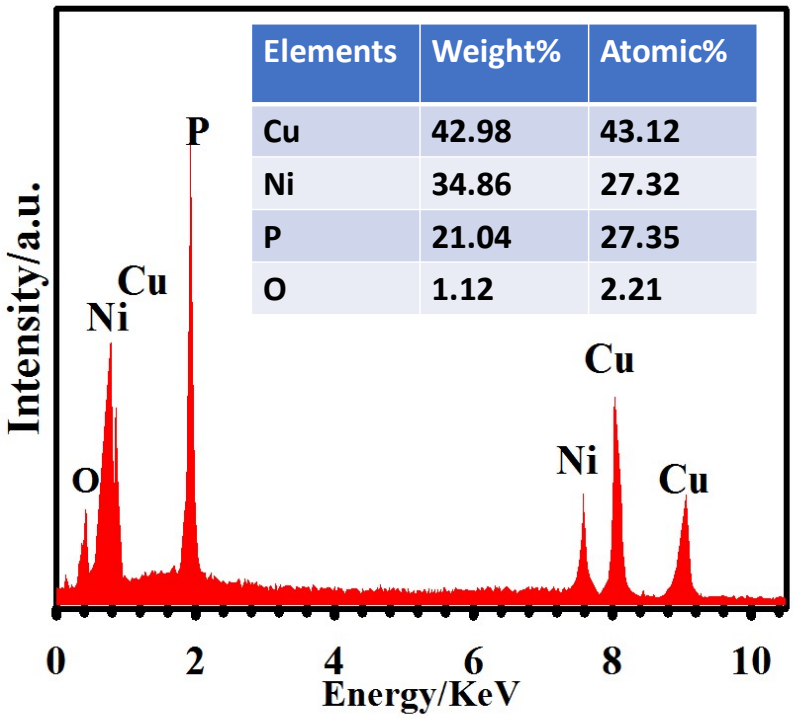

Fig. S10 EDX pattern of the NH-CNPS-350.

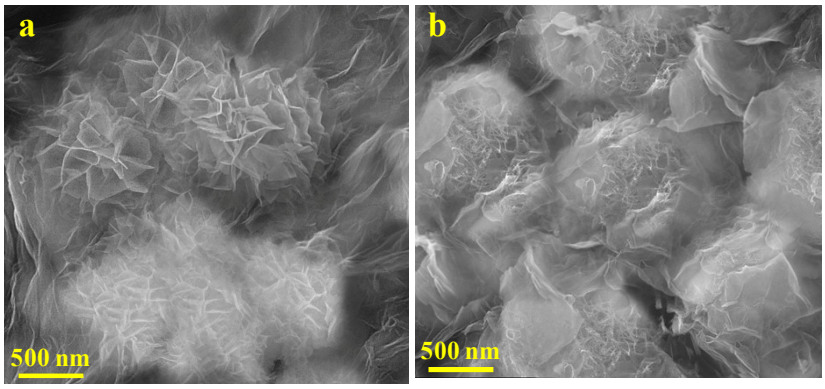

Fig. S11 (a) FE-SEM image of the NH-CNPS-rGO-1. (b) FE-SEM image of the NH-CNPS-rGO-3.

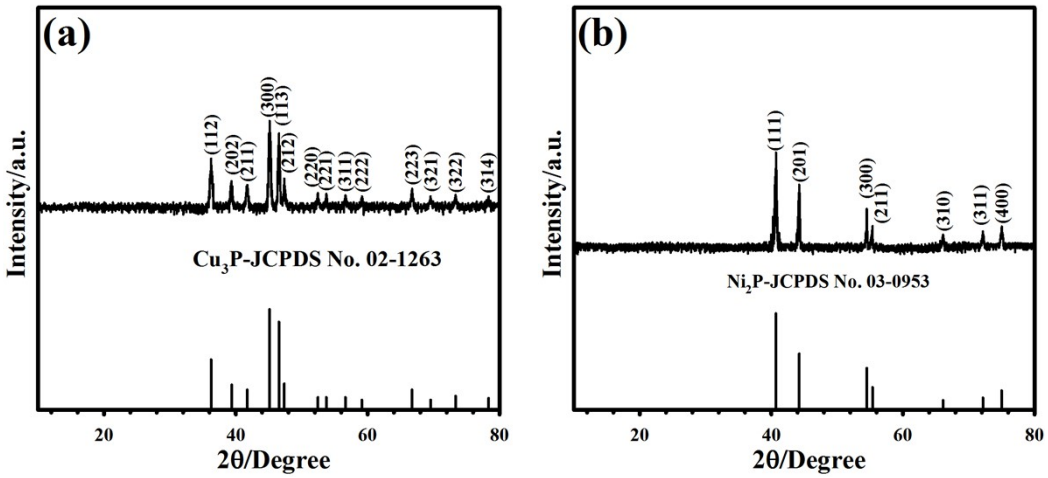

Fig. S12 (a) XRD pattern of the Cu_3P. (b) XRD pattern of the Ni_2P.

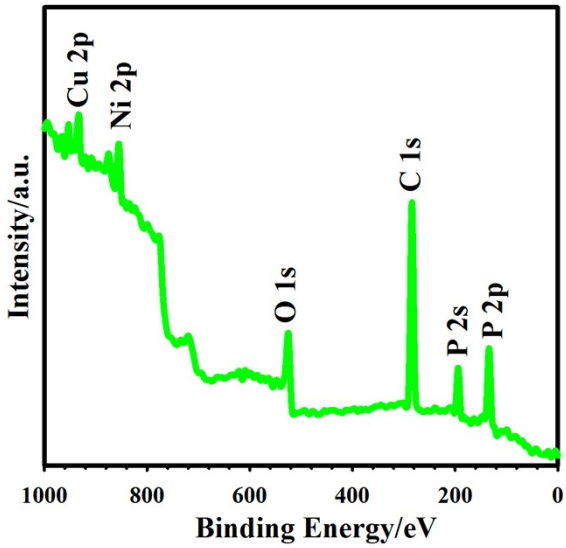

Fig. S13 Survey profile of NH-CNPS-rGO-2.

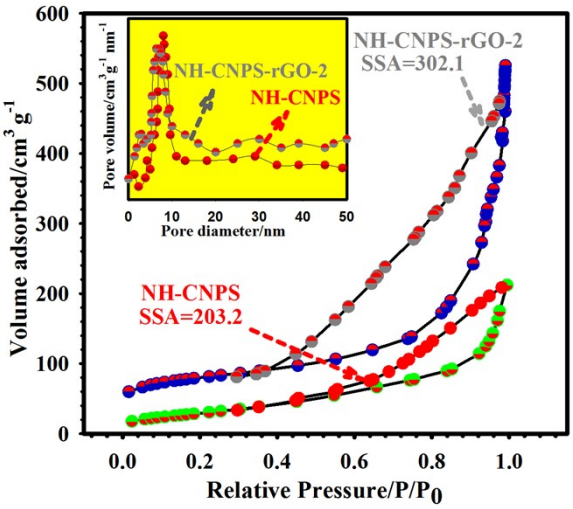

Fig. S14 (h) BET plots of the NH-CNPS-350 and NH-CNPS-rGO-2 samples and their corresponding BJH curves (inset).

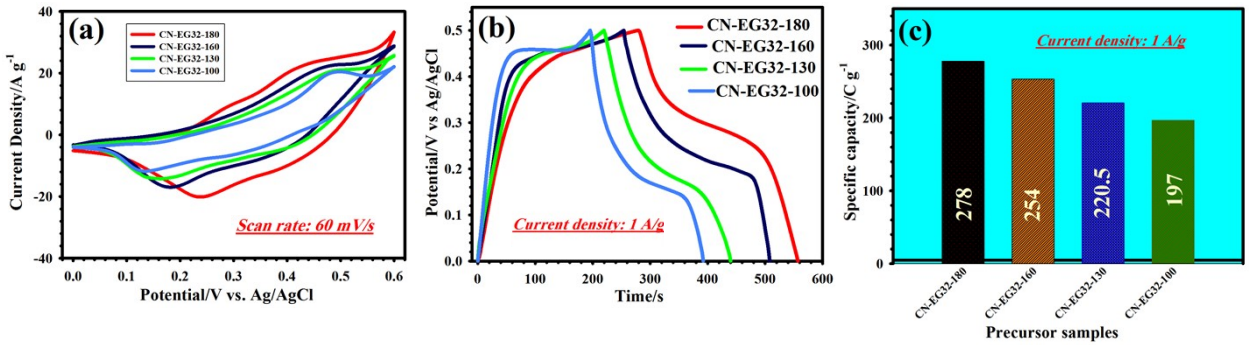

Fig. 15 (a) CV curves of the CN-EG32-180, CN-EG32-160, CN-EG32-130, and CN-EG32-100 electrodes at 60 mV/s. (b) GCD curves of the CN-EG32-180, CN-EG32-160, CN-EG32-130, and CN-EG32-100 electrodes at 1 A/g. (c) Specific capacities of CN-EG32-180, CN-EG32-160, CN-EG32-130, and CN-EG32-100 electrodes at 1 A/g.

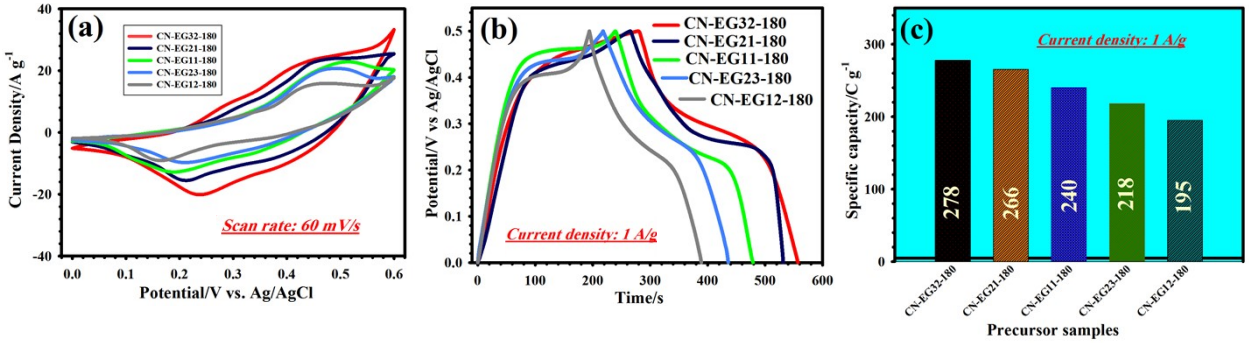

Fig. 16 (a) CV curves of the CN-EG32-180, CN-EG21-180, CN-EG11-180, CN-EG23-180, and CN-EG12-180 electrodes at 60 mV/s. (b) GCD curves of the CN-EG32-180, CN-EG21-180, CN-EG11-180, CN-EG23-180, and CN-EG12-180 electrodes at 1 A/g. (c) Specific capacities of CN-EG32-180, CN-EG21-180, CN-EG11-180, CN-EG23-180, and CN-EG12-180 electrodes at 1 A/g.

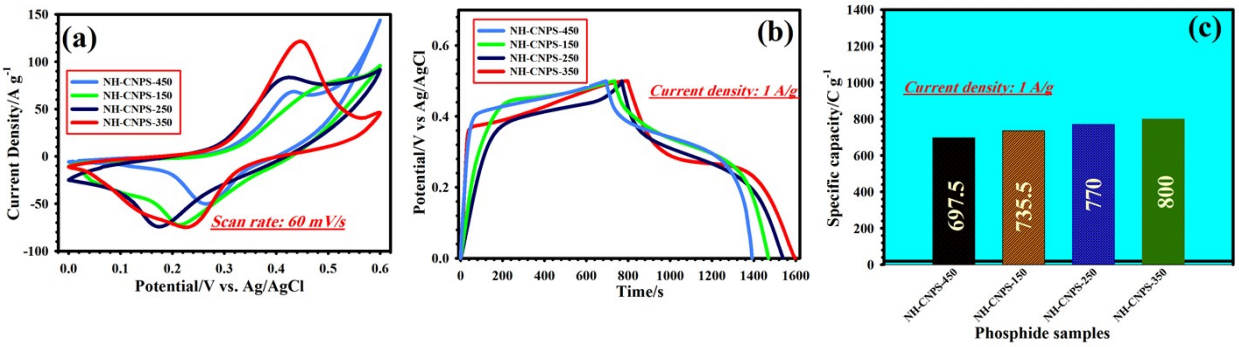

Fig. 17 (a) CV curves of the NH-CNS-150, NH-CNS-250, NH-CNS-350, and NH-CNS-450 electrodes at 60 mV/s. (b) GCD curves of the NH-CNS-150, NH-CNS-250, NH-CNS-350, and NH-CNS-450 electrodes at 1 A/g. (c) Specific capacities of NH-CNS-150, NH-CNS-250, NH-CNS-350, and NH-CNS-450 electrodes at 1 A/g.

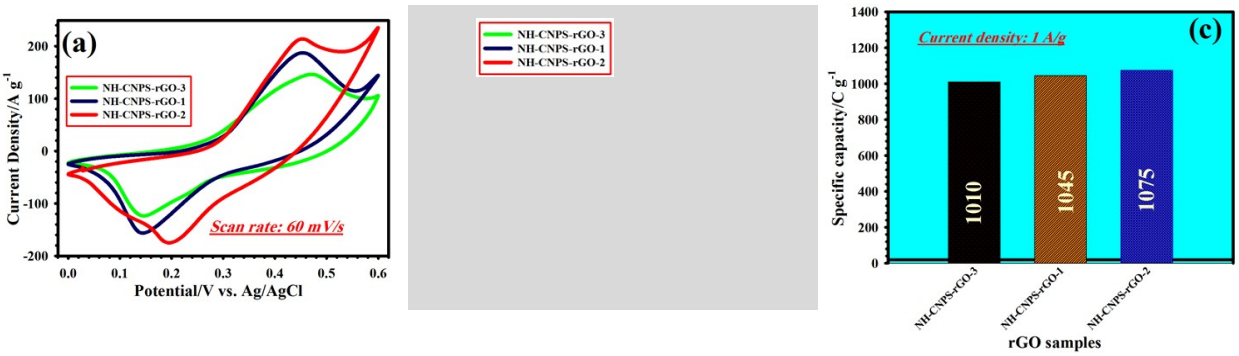

Fig. 18 (a) CV curves of the NH-CNS-rGO-1, NH-CNS-rGO-2, and NH-CNS-rGO-3 electrodes at 60 mV/s. (b) GCD curves of the NH-CNS-rGO-1, NH-CNS-rGO-2, and NH-CNS-rGO-3 electrodes at 1 A/g. (c) Specific capacities of NH-CNS-rGO-1, NH-CNS-rGO-2, and NH-CNS-rGO-3 electrodes at 1 A/g.

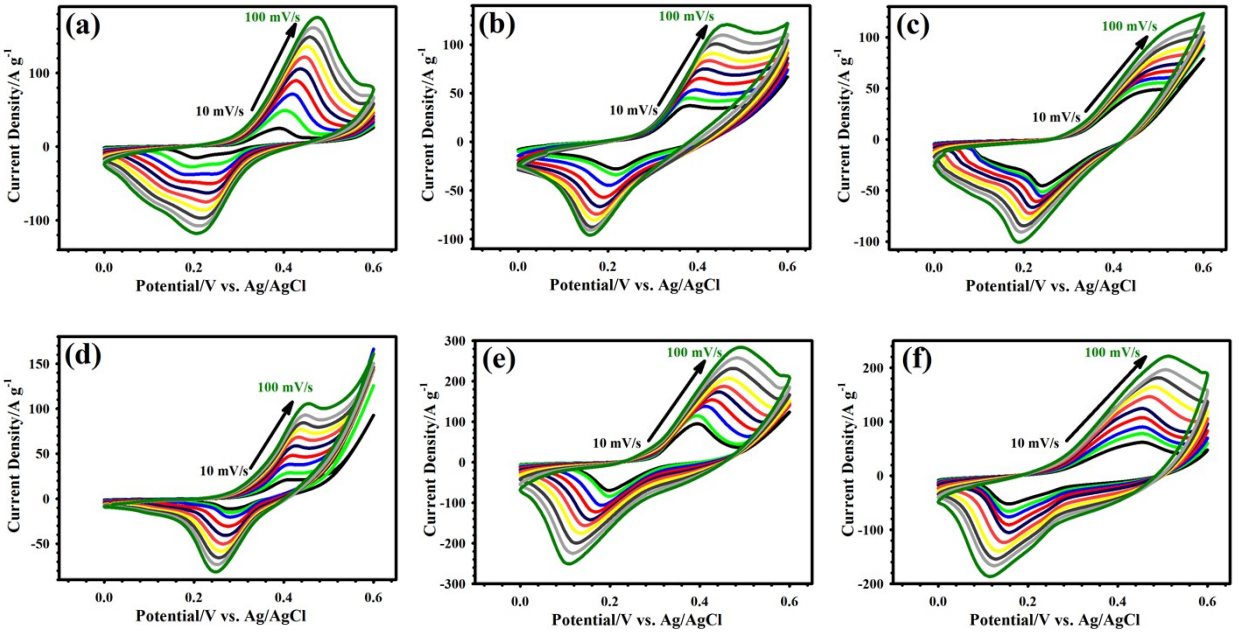

Fig. S19 (a) CV curves of the NH-CNS-350 electrode at various scan rates from 10 to 100 mV/s. (b) CV curves of the NH-CNS-250 electrode at various scan rates from 10 to 100 mV/s. (c) CV curves of the NH-CNS-150 electrode at various scan rates from 10 to 100 mV/s. (d) CV curves of the NH-CNS-450 electrode at various scan rates from 10 to 100 mV/s. (e) CV curves of the NH-CNS-rGO-1 electrode at various scan rates from 10 to 100 mV/s. (f) CV curves of the NH-CNS-rGO-3 electrode at various scan rates from 10 to 100 mV/s.

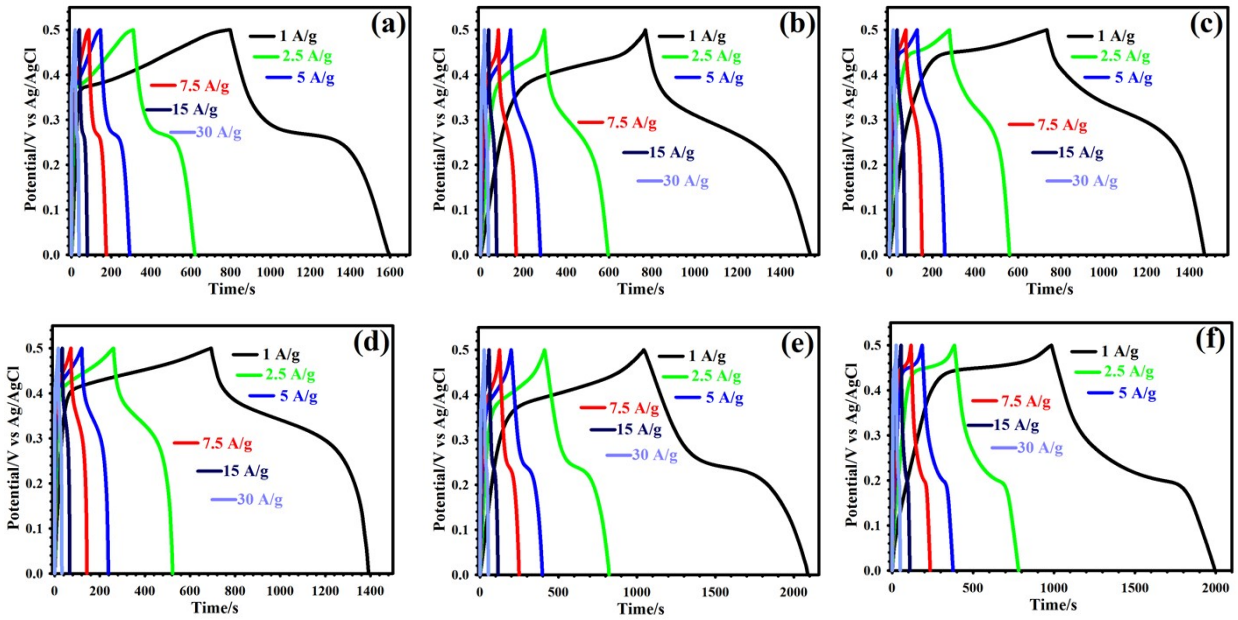

Fig. S20 (a) GCD curves of the NH-CNS-350 electrode from 1 to 30 A/g. (b) GCD curves of the NH-CNS-250 electrode from 1 to 30 A/g. (c) GCD curves of the NH-CNS-150 electrode from 1 to 30 A/g. (d) GCD curves of the NH-CNS-450 electrode from 1 to 30 A/g. (e) GCD curves of the NH-CNS-rGO-1 electrode from 1 to 30 A/g. (f) GCD curves of the NH-CNS-rGO-3 electrode from 1 to 30 A/g.

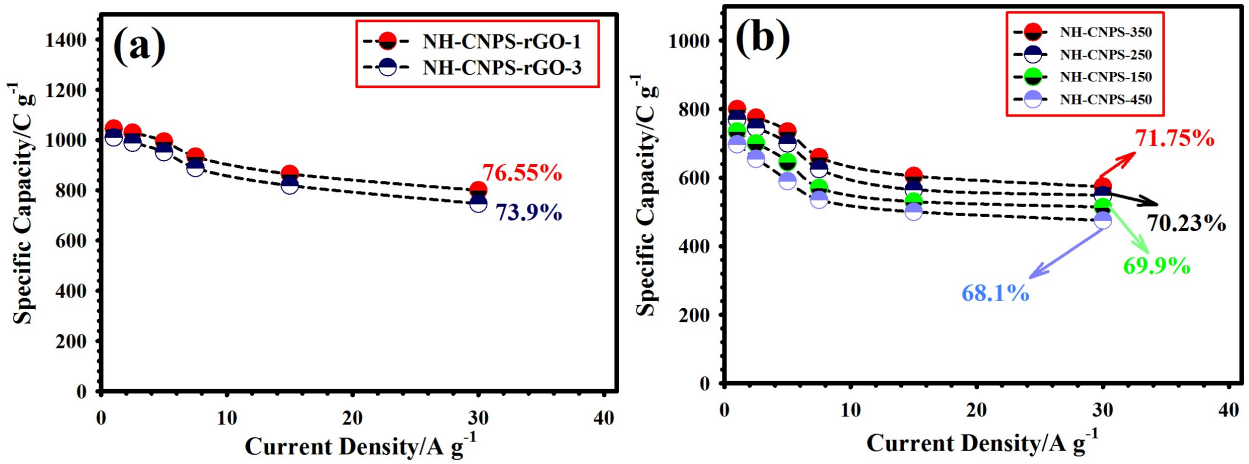

Fig. S21 (a) Specific capacities vs. current densities of the NH-CNPS-rGO-1 and NH-CNPS-rGO-3. (b) Specific capacities vs. current densities of the NH-CNPS-150, NH-CNPS-250, NH-CNPS-350, and NH-CNPS-450.

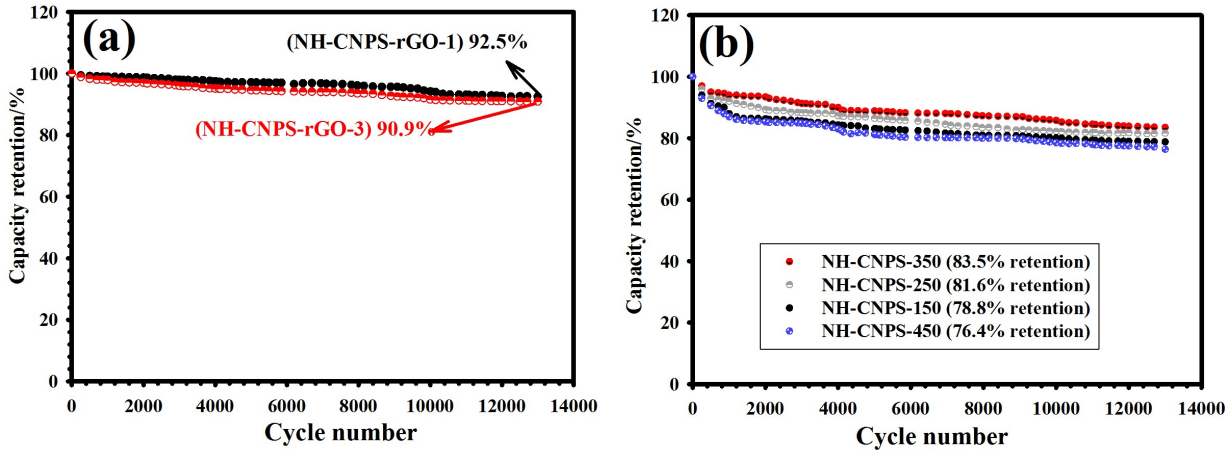

Fig. S22 (a) Durability of the NH-CNPS-rGO-1 and NH-CNPS-rGO-3 electrodes at 15 A/g. (b) Durability of the NH-CNPS-150, NH-CNPS-250, NH-CNPS-350, and NH-CNPS-450electrodes at 15 A/g.

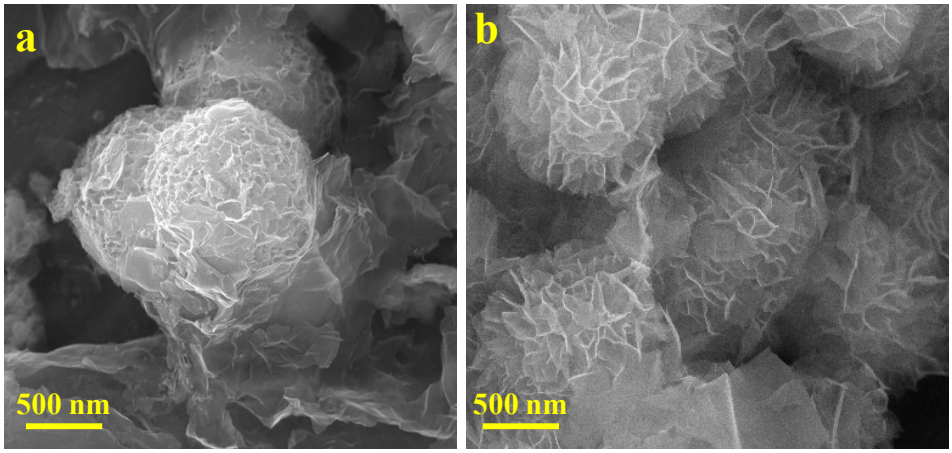

Fig. S23 (a) FE-SEM images of the NH-CNPS-rGO-2 after 13000 GCD cycles. (b) FE-SEM images of the NH-CNPS-350 after 13000 GCD cycles.

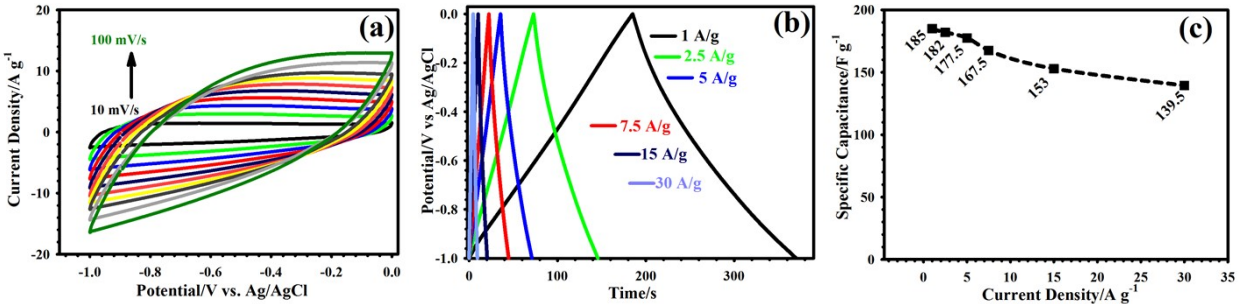

Fig. S24 (a) CVs of the AC electrode from 10 to 100 mV/s. (b) GCD graphs of the AC from 1 to 30 A/g. (c) Specific capacities vs. current densities of the AC electrode.

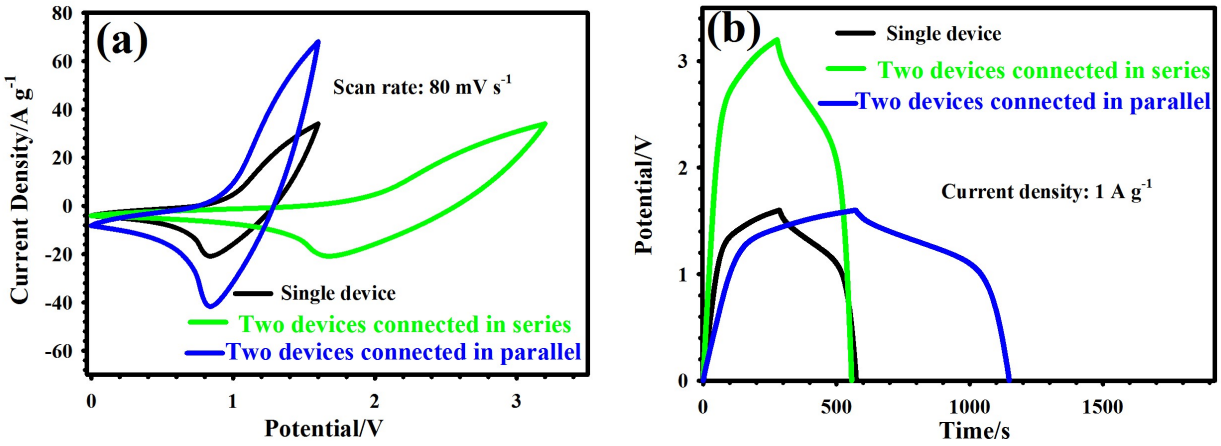

Fig. S25 (a) CV curves of single and two devices connected in series and parallel at scan rate of 80 mV/s. (b) GCD curves of single and two devices connected in series and parallel at 1 A g^{-1}.

Table S1. The as-synthesized precursors and their corresponding synthesis parameters

Entry	Starting materials	Solvothermal Temperature (°C)	Solvothermal Time (h)	mmol ratios of the $Cu(CH_3COO)_2$:$Ni(CH_3COO)_2$	Final precursors
1	CuNi-EG	100	10	3:2	CN-EG32-100
2	CuNi-EG	130	10	3:2	CN-EG32-130
3	CuNi-EG	160	10	3:2	CN-EG32-160
4	CuNi-EG	180	10	3:2	CN-EG32-180 (Optimized sample)

Table S2. The as-synthesized precursors and their corresponding synthesis parameters

Entry	Starting materials	Solvothermal Temperature (°C)	Solvothermal Time (h)	mmol ratios of the $Cu(CH_3COO)_2$:$Ni(CH_3COO)_2$	Final precursors
1	CuNi-EG	180	10	1:1	CN-EG11-180
2	CuNi-EG	180	10	1:2	CN-EG12-180
3	CuNi-EG	180	10	2:1	CN-EG21-180
4	CuNi-EG	180	10	2:3	CN-EG23-180
5	CuNi-EG	180	10	3:2	CN-EG32-180 (Optimized sample)

Table S3. The as-synthesized phosphide samples and their corresponding synthesis parameters

Entry	Starting materials	Phosphorization Temperature (°C)	Phosphorization Time (h)	Final samples
1	CN-EG180	150	2	NH-CNPS-150
2	CN-EG180	250	2	NH-CNPS-250
3	CN-EG180	350	2	NH-CNPS-350 (Optimized sample)
4	CN-EG180	450	2	NH-CNPS-450

Table S4. Comparison of the performance of the NH-CNPS-rGO-2 with other previously reported materials.

Composition	Capacity (C/g)	Cycles, retention	Rate capability	ED (Wh kg^{-1})	Reference
NiCoP	**761 at 1 A g^{-1}**	**50000, 90.2%**	**91.1% at 20 A g^{-1}**	**35.6**	**1**
Ni_2P/NiCoP	**741.3 at 1 A g^{-1}**	**30000, 89.2%**	**75.5% at 50 A g^{-1}**	**44.5**	**2**
Ni–Co–P/POx/C	**583 at 1 A g^{-1}**	**5000, 77.3%**	**62.7% at 30 A g^{-1}**	**37.59**	**3**
O-Co_xNi_yP	**717.1 at 1 A g^{-1}**	**5000, 95.1%**	**66.7% at 20 A g^{-1}**	**47.5**	**4**
Ni_2P/Ni/C	**257.2 at 1 A g^{-1}**	**5000, 84.3%**	**60.5% at 10 A g^{-1}**	**25.4**	**5**
Mn-CoP/NF	**456 at 0.5 A g^{-1}**	**20000, 89%**	**77.4% at 10 A g^{-1}**	**14.82**	**6**

Ni2P/Co_3O_4/N-CQDs	**1044 at 1 A g^{-1}**	**6000, 90.5%**	**83.9% at 20 A g^{-1}**	**53.5**	**7**
PPy@CoP	**443 at 1 A g^{-1}**	**5000, 93%**	**50.5% at 20 A g^{-1}**	**38.1**	**8**
NH-CNPS-rGO-2	**1075 at 1 A g^{-1}**	**13000, 94.7%**	**79.3% at 30 A g^{-1}**	**64**	**This study**

References

1 M. Gao, W.-K. Wang, X. Zhang, J. Jiang and H.-Q. Yu, *J. Phys. Chem. C* 2018, **122**, 25174–25182.

2 Z. Li, K. Ma, F. Guo, C. Ji, H. Mi, P. Qiu and H. Pang, *Mater. Lett*. 2021, **288**, 129319.

3 X. Zhang, J. Wang, Y. Sui, F. Wei, J. Qi, Q. Meng, Y. He and D. Zhuang, *ACS Appl. Nano Mater*. 2020, **3**, 11945–11954.

4 S. Jiang, M. Pang, R. Liu, J. Song, R. Wang, N. Li, Q. Pan, H. Yang, W. He and J. Zhao, *J. Alloys Compd.* 2022, **895**, 162451.

5 Y. Xu, S. Xiong, S. Weng, J. Wang, J. Wang, H. Lin, Y. Jiao and J. Chen, *New J. Chem*., 2020, **44**, 6810-6817.

6 M. Zhang, H. Du, Z. Wei, X. Zhang and R. Wang, *ACS Appl. Energy Mater*. 2022, **5**, 186–195

7 Z. Ji, K. Liu, L. Chen, Y. Nie, D. Pasang, Q. Yu, X. Shen, K. Xu and S. Premlatha, *J. Colloid Interface Sci*. 2022, **609**, 503-512.

8 C. Yue, B. Hu, W. Huang, A. Liu, Z. Guo, J. Mu, X. Zhang, X. Liu and H. Che, *J. Electroanal. Chem*. 2021, **899**, 115656.